Syntheses and Structures of the New Quaternary Group IV Tellurides $Cs_{0.68}CuTiTe_4$ and $Cs_3CuHf_2Te_{10}$

Michael F. Mansuetto, Jason A. Cody, Samson Chien, and James A. Ibers

Department of Chemistry, Northwestern University, Evanston, Illinois 60208-3113

Received November 4, 1994. Revised Manuscript Received February 28, 1995[⊗]

The new compounds $Cs_{0.68}CuTiTe_4$ and $Cs_3CuHf_2Te_{10}$ have been synthesized at 350 and 475 °C, respectively, through reaction of the elements with a Cs_2Te_n flux. $Cs_{0.68}CuTiTe_4$ crystallizes in space group C_{2h}^3–$C2/m$ of the monoclinic system with four formula units in a cell of dimensions $a = 19.728(11)$, $b = 3.923(2)$, $c = 13.374(7)$ Å, $\beta = 129.65(1)°$, $V = 796.9(7)$ Å^3 ($T = 113$ K). $Cs_3CuHf_2Te_{10}$ crystallizes in space group C_i^1–$P\bar{1}$ of the triclinic system with two formula units in a cell of dimensions $a = 9.889(5)$, $b = 10.916(6)$, $c = 11.110(6)$ Å, $\alpha = 92.08(1)$, $\beta = 90.15(1)$, $\gamma = 101.27(1)°$, $V = 1175.3(11)$ Å^3 ($T = 113$ K). The structures of both compounds have been determined by single-crystal X-ray methods. $Cs_{0.68}CuTiTe_4$ has a three-dimensional channel structure. Cs^+ cations occupy the channels. The channels are built up from layers that are interconnected by Te–Te bonds. In these layers there are *pairs* of edge-shared $CuTe_4$ tetrahedra that in turn edge-share to $TiTe_6$ octahedra. The conductivity in the needle (b) direction is 5×10^{-3} Ω^{-1}cm^{-1} at room temperature. The structure of $Cs_3CuHf_2Te_{10}$ comprises infinite one-dimensional chains of $HfTe_7$ polyhedra and edge-shared $CuTe_4$ tetrahedra; these chains are separated from one another by Cs^+ cations. A chain may be formulated as $^1_\infty[CuHf_2(Te_3)(Te_2)_3(Te)^{3-}]$. The conductivity in the needle [11$\bar{1}$] direction is $<1 \times 10^{-5}$ Ω^{-1}cm^{-1} at room temperature.

Introduction

The reactive flux method[1] has afforded an amazing variety of structure types among new ternary and quaternary metal chalcogenides and polychalcogenides. These include isolated,[2] one-dimensional,[1,3–8] two-dimensional,[9–11] and three-dimensional[7,12,13] species. The wide variety of structure types may be attributed to the propensity of chalcogen atoms to form Q–Q bonds (Q = S, Se, Te). While the majority of species synthesized have been sulfides or selenides, the reactive flux method has been applied to the synthesis of tellurides.[4,8,14] Although a few ternary cesium tellurides are known,[15–20] only $Cs_4Zr_3Te_{16}$[8] was prepared by the reactive flux method. It appears that the use of Cs, rather than the more typical Na or K, in the reactive flux leads to a wide variety of new compounds. We illustrate this here with the syntheses and structures of two new cesium tellurides, the three-dimensional channel compound $Cs_{0.68}CuTiTe_4$[21] and the one-dimensional chain compound $Cs_3CuHf_2Te_{10}$.

Experimental Section

Syntheses. $Cs_{0.68}CuTiTe_4$ was synthesized by combining Cs_2Te_3 (107 mg, 0.17 mmol) with powders of the elements Cu (21 mg, 0.33 mmol; Aldrich, 99.999%), Ti (16 mg, 0.33 mmol; AESAR, 99.9%), and Te (106 mg, 0.83 mmol; Aldrich, 99.8%). $Cs_3CuHf_2Te_{10}$ was synthesized by combining Cs_2Te_3 (158 mg, 0.24 mmol) with powders of the elements Cu (8 mg, 0.12 mmol), Hf (22 mg, 0.12 mmol; Johnson-Matthey, 99.6%), and Te (62 mg, 0.49 mmol). The binary starting material Cs_2Te_3 was synthesized by reaction of Cs (Aldrich 99.5%) with Te in stoichiometric quantities in liquid ammonia under an Ar atmosphere. The composition Cs_2Te_3 was confirmed by comparison of its powder diffraction pattern with that generated from the known structure.[22,23]

The reaction mixtures were loaded into fused silica tubes in a drybox under an Ar atmosphere. The tubes were evacuated to approximately 10^{-3} Torr and sealed. For $Cs_{0.68}CuTiTe_4$ the tube was heated in a furnace at 350 °C for 4 days before being cooled at 4 °C/h to room temperature. For $Cs_3CuHf_2Te_{10}$ the tube was heated at 475 °C for 6 days before being cooled at 4 °C/h to room temperature. Black needles of $Cs_{0.68}CuTiTe_4$ were manually extracted from the melt while black needles of $Cs_3CuHf_2Te_{10}$ were isolated by washing the

[⊗] Abstract published in *Advance ACS Abstracts,* April 1, 1995.

(1) Sunshine, S. A.; Kang, D.; Ibers, J. A. *J. Am. Chem. Soc.* **1987**, *109*, 6202–6204.
(2) Schreiner, S.; Aleandri, L. E.; Kang, D.; Ibers, J. A. *Inorg. Chem.* **1989**, *28*, 392–393.
(3) Kang, D.; Ibers, J. A. *Inorg. Chem.* **1988**, *27*, 549–551.
(4) Keane, P. M.; Ibers, J. A. *Inorg. Chem.* **1991**, *30*, 1327–1329.
(5) Kanatzidis, M. G.; Park, Y. *J. Am. Chem. Soc.* **1989**, *111*, 3767–3769.
(6) Park, Y.; Kanatzidis, M. G. *Angew. Chem., Int. Ed. Engl.* **1990**, *29*, 914–915.
(7) Kanatzidis, M. G. *Chem. Mater.* **1990**, *2*, 353–363.
(8) Cody, J. A.; Ibers, J. A. *Inorg. Chem.* **1994**, *33*, 2713–2715.
(9) Mansuetto, M. F.; Keane, P. M.; Ibers, J. A. *J. Solid State Chem.* **1992**, *101*, 257–264.
(10) Mansuetto, M. F.; Keane, P. M.; Ibers, J. A. *J. Solid State Chem.* **1993**, *105*, 580–587.
(11) Lu, Y.-J.; Ibers, J. A. *J. Solid State Chem.* **1991**, *94*, 381–385.
(12) Keane, P. M.; Ibers, J. A. *J. Solid State Chem.* **1991**, *93*, 291–297.
(13) Keane, P. M.; Ibers, J. A. *Inorg. Chem.* **1991**, *30*, 3096–3098.
(14) Park, Y.; Degroot, D. C.; Schindler, J.; Kannewurf, C. R.; Kanatzidis, M. G. *Angew. Chem., Int. Ed. Engl.* **1991**, *30*, 1325–1328.
(15) Brinkmann, C.; Eisenmann, B.; Schäfer, H. *Mater. Res. Bull.* **1985**, *20*, 1207–1211.
(16) Brinkmann, C.; Eisenmann, B.; Schäfer, H. *Mater. Res. Bull.* **1985**, *20*, 299–307.
(17) Bronger, W.; Kathage, H. U. *J. Alloys Compd.* **1992**, *184*, 87–94.
(18) Eisenmann, B.; Jäger, J. *Z. Kristallogr.* **1991**, *197*, 251–252.
(19) Eisenmann, B.; Jäger, J. *Z. Kristallogr.* **1991**, *197*, 253–254.
(20) Bronger, W.; Kimpel, M.; Schmitz, D. *Acta Crystallogr., Sect. B: Struct. Sci.* **1983**, *39*, 235–238.
(21) Cody, J. A.; Mansuetto, M. F.; Chien, S.; Ibers, J. A. *Mater. Sci. Forum* **1994**, *152–153*, 35–42.
(22) Böttcher, P. *J. Less-Common Met.* **1980**, *70*, 263–271.
(23) Yvon, K.; Jeitschko, W.; Parthé, E. *J. Appl. Crystallogr.* **1977**, *10*, 73–74.

0897-4756/95/2807-0894$09.00/0

Table 1. Crystallographic Details for $Cs_{0.68}CuTiTe_4$ and $Cs_3CuHf_2Te_{10}$

formula	$Cs_{0.68}CuTiTe_4$	$Cs_3CuHf_2Te_{10}$
fw	712.6	2095.3
space group	C_{2h}^3–$C2/m$	C_i^1–$P\bar{1}$
a (Å)	19.728(11)	9.889(5)
b (Å)	3.923(2)	10.916(6)
c (Å)	13.374(7)	11.110(6)
α, deg	90	92.08(1)
β, deg	129.65(1)	90.15(1)
γ, deg	90	101.27(1)
V (Å^3)	796.9(7)	1175.3(11)
Z	4	2
ϱ_{calcd} (g cm^{-3})	5.94	5.92
T (K)[a]	113	113
μ (cm^{-1})	209.9	264.3
transmission factors	0.564–0.684	0.457–0.577
R (on F for $F_o^2 > 2\sigma(F_o^2)$)[b]	0.029	0.063
$R_w(F^2)$[b]	0.071	0.128

[a] The low-temperature system is based on a design by Huffman.[32] [b] $R(F_o) = \Sigma||F_o| - |F_c||/\Sigma|F_o|$; $R_w(F_o^2) = \{\Sigma[w(F_o^2 - F_c^2)^2]/\Sigma wF_o^4\}^{1/2}$, $w^{-1} = \sigma^2(F_o^2) + (0.04F_o^2)^2$; $w^{-1} = \sigma^2(F_o^2)$, $F_o^2 < 0$.

excess flux away with water. The yield of both reactions was very low (ca. 10 crystals of reasonable size (0.3 mm) per good tube.) Major products, in addition to the melt, include amorphous material and a few crystals of what could be $CsCuMTe_3$ phases on the basis of EDAX results. The compounds are stable in air and water. The quaternary nature of the compounds and approximate atomic ratios (1:1:1:3 for $Cs_{0.68}CuTiTe_4$ and 2:1:2:12 for $Cs_3CuHf_2Te_{10}$) were determined with the microprobe of an EDAX (energy-dispersive analysis by X-rays) equipped Hitachi S-570 scanning electron microscope. In both instances, the ratios were consistent from crystal to crystal, batch to batch. The final formulations of the compounds are based on the X-ray structure determinations.

Crystallography. Cell parameters were determined from a least-squares analysis of the setting angles of 29 reflections in the range $13° < 2\theta(\text{Mo K}\alpha_1) < 33°$ for $Cs_{0.68}CuTiTe_4$ and 25 refections in the range $25° < 2\theta(\text{Mo K}\alpha_1) < 35°$ for $Cs_3CuHf_2Te_{10}$ that had been automatically centered at 113 K on a Picker diffractometer operated from a PC.[24] Six representative standard reflections monitored every 100 refections showed no significant variations in intensity during either data collection. Crystallographic details are listed in Table 1. Additional information is given in Table SI (supplementary material).[25] Intensity data were processed and corrected for absorption[26] on an IBM RS/6000 series computer with programs and methods standard in this laboratory.

For $Cs_{0.68}CuTiTe_4$ the observed Laue symmetry and the systematic absences are consistent with the monoclinic space groups C_2^3–C2, C_s^3–Cm, and C_{2h}^3–$C2/m$. Analysis of the data with the program XPREP[27] favored the centrosymmetric space group $C2/m$. The structure was solved in this space group with the direct methods program XS of the SHELXTL PC program package.[27] The structure of $Cs_3CuHf_2Te_{10}$ was solved with the use of the direct methods program SHELX-86.[28] The structures were refined by full-matrix least-squares techniques with the use of the program SHELXL-93,[29] the function $\Sigma w(F_o^2 - F_c^2)^2$ being minimized. Prior to the refinement of its occupancy, the Cs position in $Cs_{0.68}CuTiTe_4$ displayed excessive thermal motion. The final refinement led to a value of $R_w(F_o^2)$ of 0.071. The conventional R index (on F for $F_o^2 > 2\sigma(F_o^2)$) is

(24) Huffman, J. C.; Streib, W. E. Unpublished work.
(25) Supplementary material.
(26) de Meulenaer, J.; Tompa, H. *Acta Crystallogr.* **1965**, *19*, 1014–1018.
(27) Sheldrick, G. M. SHELXTL PC Version 4.1 An integrated system for solving, refining, and displaying crystal structures from diffraction data. Siemens Analytical X-Ray Instruments, Inc. Madison, WI.
(28) Sheldrick, G. M. In *Crystallographic Computing 3*; Sheldrick, G. M., Krüger, C., Goddard, R., Eds.; Oxford University Press: London, 1985; pp 175–189.
(29) Sheldrick, G. M. *J. Appl. Crystallogr.*, in press.

Table 2. Atomic Coordinates ($\times 10^4$) and Equivalent Isotropic Displacement Parameters (Å$^2 \times 10^3$) for $Cs_{0.68}CuTiTe_4$

	x	y	z	U(eq)[a]
Cs	105(1)	0	3632(1)	23(1)
Cu	2427(1)	0	666(1)	10(1)
Ti	2998(1)	0	8049(2)	7(1)
Te(1)	782(1)	0	1472(1)	7(1)
Te(2)	3091(1)	0	6010(1)	8(1)
Te(3)	3701(1)	0	509(1)	8(1)
Te(4)	3264(1)	0	3129(1)	8(1)

[a] U(eq) is defined as one-third of the trace of the orthogonalized U_{ij} tensor.

Table 3. Atomic Coordinates ($\times 10^4$) and Equivalent Isotropic Displacement Parameters (Å$^2 \times 10^3$) for $Cs_3CuHf_2Te_{10}$

	x	y	z	U(eq)
Cs(1)	8859(2)	1096(2)	2621(2)	19(1)
Cs(2)	4461(2)	2371(2)	3921(2)	21(1)
Cs(3)	3006(2)	3769(2)	−1047(2)	20(1)
Cu	−839(4)	6280(3)	5572(3)	17(1)
Hf(1)	1074(1)	6207(1)	3640(1)	14(1)
Hf(2)	3087(1)	8414(1)	1443(1)	13(1)
Te(1)	−1601(2)	4382(2)	3943(2)	13(1)
Te(2)	−756(2)	7976(2)	4050(2)	14(1)
Te(3)	1944(2)	4048(2)	2370(2)	15(1)
Te(4)	2105(2)	8868(2)	3955(2)	14(1)
Te(5)	771(2)	6349(2)	1035(2)	12(1)
Te(6)	3948(2)	6400(2)	2905(2)	14(1)
Te(7)	378(2)	8748(2)	661(2)	14(1)
Te(8)	5344(2)	9116(2)	3052(2)	18(1)
Te(9)	3323(2)	10913(2)	703(2)	14(1)
Te(10)	4073(2)	7514(2)	−758(2)	14(1)

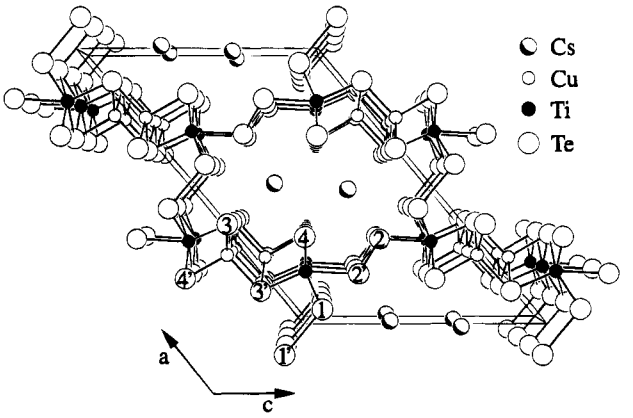

Figure 1. View of the structure of $Cs_{0.68}CuTiTe_4$ down [010] with atoms labeled. Here and in succeeding figures the atoms are drawn as circles of arbitrary size.

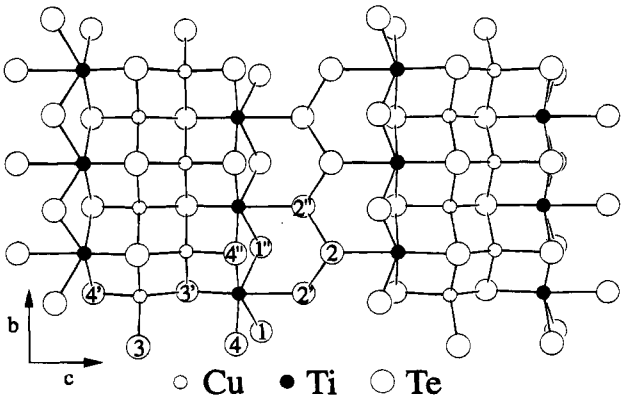

Figure 2. View of the structure of $Cs_{0.68}CuTiTe_4$ down a^* with atoms labeled.

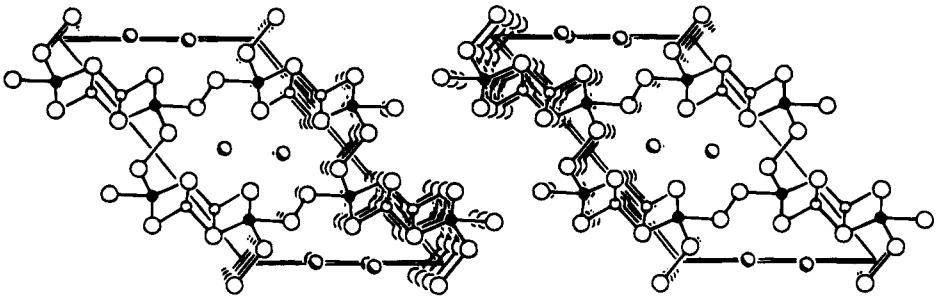

Figure 3. Stereoview of the structure of $Cs_{0.68}CuTiTe_4$.

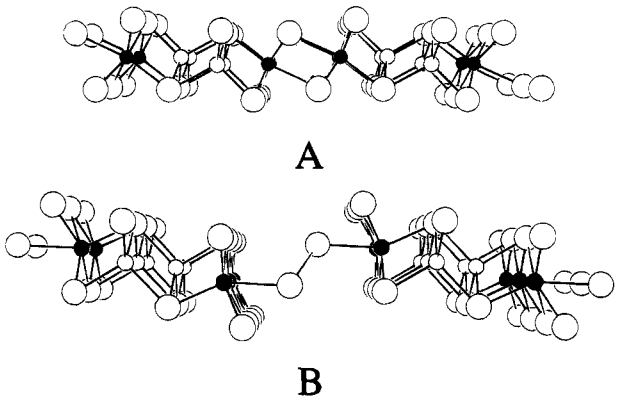

Figure 4. Comparison of a layer of $NaCuTiS_3$ (**A**) with a pseudolayer of $Cs_{0.68}CuTiTe_4$ (**B**).

0.029. The final difference electron density map shows no features with a height greater than 0.7% that of a Te atom. For $Cs_3CuHf_2Te_{10}$ the final refinement led to a value of $R_w(F_o^2)$ of 0.128. The conventional R index (on F for $F_o^2 > 2\sigma(F_o^2)$) is 0.063. The final difference electron density map shows no features with a height greater than 1.8% that of a Hf atom.

Values of the atomic parameters and equivalent isotropic displacement parameters are given in Tables 2 and 3 for $Cs_{0.68}CuTiTe_4$ and $Cs_3CuHf_2Te_{10}$, respectively. The anisotropic displacement parameters are presented in Tables SII and SIII.[25]

Results

$Cs_{0.68}CuTiTe_4$. $Cs_{0.68}CuTiTe_4$ is a new member of a growing family of quaternary A/Cu/M/Q compounds, where A = alkali metal, M = group IV element, and Q = chalcogen.[9,10] Since the structure of the $ACuMQ_3$ series changes on going from A = K[9] to A = Na,[10] we anticipated the formation of $CsCuMTe_3$ with yet a different structure. Instead $Cs_{0.68}CuTiTe_4$ formed. $Cs_{0.68}CuTiTe_4$ has a three-dimensional channel structure. The channels are built up from layers that are interconnected by Te–Te bonds. The Te(1)–Te(1′) bond of 3.084 (2) Å lies in the *ac* plane, as seen in Figure 1. The ···Te(2)–Te(2′)–Te(2″)··· bonds of 2.923(1) Å form an infinite zigzag chain along *b* (Figure 2). Within the channels the Cs^+ cations, which occupy two out of every three Cs sites, are coordinated by nine Te atoms in a monocapped square-prismatic arrangement. A stereo view of the structure is given in Figure 3. Selected distances and angles are given in Table 4. Complete metrical data are given in Table SIV.[25] The layers contain *pairs* of $CuTe_4$ tetrahedra joined at the Te(3)–Te(3′) edge, and these tetrahedra are in turn joined at the Te(3)–Te(4) edge to $TiTe_6$ octahedra. The units are further connected through Te(1)–Te(1′) bonds and Te(2)–Te(2′) bonds (Figures 1 and 2) to complete the channel structure. The Cu–Te bond distances range from 2.575(2) to 2.653(2) Å and are in good agreement with those found in Cu_2MTe_3 (2.594(1) to 2.705(1) Å).[12] The $CuTe_4$ tetrahedron is distorted with Te–Cu–Te bond angles ranging from 97.51(6) to 116.06(5)°. The Ti–Te distances range from 2.632(2) to 2.846(2) Å; the Ti–Te distance in $TiTe_2$ is 2.769(1) Å.[30] The $TiTe_6$

Table 4. Selected Bond Lengths (Å) and Angles (deg) for $Cs_{0.68}CuTiTe_4$[a]

Cs–Te(3)#1	3.769(2)
Cs–Te(4)#1	3.790(2)
Cs–Te(2)#2	3.818(2)
Cs–Te(4)#2	3.896(2)
Cu–Te(4)	2.575(2)
Cu–Te(3)#3	2.609(1)
Cu–Te(3)	2.653(2)
Cu–Cu#3	2.786(2)
Cu–Ti#2	3.057(2)
Ti–Te(3)#4	2.632(2)
Ti–Te(4)#5	2.743(2)
Ti–Te(1)#2	2.843(2)
Ti–Te(2)	2.846(2)
Te(1)–Te(1)#6	3.084(2)
Te(2)–Te(2)#5	2.923(1)
Te(3)#1–Cs–Te(3)#7	62.72(4)
Te(3)#1–Cs–Te(4)#1	65.84(3)
Te(3)#7–Cs–Te(4)#1	97.44(4)
Te(4)#1–Cs–Te(4)#7	62.33(4)
Te(3)#1–Cs–Te(2)#2	111.90(4)
Te(3)#7–Cs–Te(2)#2	80.70(4)
Te(4)#1–Cs–Te(2)#2	177.64(3)
Te(4)#7–Cs–Te(2)#2	117.87(4)
Te(2)#2–Cs–Te(2)#5	61.82(4)
Te(3)#1–Cs–Te(1)	62.17(5)
Te(4)#1–Cs–Te(1)	127.85(3)
Te(2)#2–Cs–Te(1)	49.97(3)
Te(3)#1–Cs–Te(4)#2	174.80(4)
Te(3)#7–Cs–Te(4)#2	118.15(4)
Te(4)#1–Cs–Te(4)#2	118.43(4)
Te(4)#7–Cs–Te(4)#2	87.42(4)
Te(2)#2–Cs–Te(4)#2	63.86(4)
Te(2)#5–Cs–Te(4)#2	94.40(4)
Te(1)–Cs–Te(4)#2	113.29(5)
Te(4)#2–Cs–Te(4)#5	60.46(4)
Te(4)–Cu–Te(3)#3	112.02(4)
Te(3)#8–Cu–Te(3)#3	97.51(6)
Te(4)–Cu–Te(3)	103.56(6)
Te(3)#3–Cu–Te(3)	116.06(5)
Te(3)#4–Ti–Te(4)#5	106.18(5)
Te(4)#5–Ti–Te(4)#2	91.29(7)
Te(3)#4–Ti–Te(1)#2	91.32(5)
Te(4)#5–Ti–Te(1)#2	161.95(8)
Te(4)#2–Ti–Te(1)#2	87.94(5)
Te(1)#2–Ti–Te(1)#5	87.27(7)
Te(3)#4–Ti–Te(2)	153.25(8)
Te(4)#5–Ti–Te(2)	92.27(6)
Te(1)#2–Ti–Te(2)	69.75(5)
Te(2)#2–Te(2)–Te(2)#5	84.31(5)

[a] Symmetry transformations used to generate equivalent atoms: #1 $x - 1/2, y - 1/2, z$; #2 $-x + 1/2, -y + 1/2, -z + 1$; #3 $-x + 1/2, -y + 1/2, -z$; #4 $x, y, z + 1$; #5 $-x + 1/2, -y - 1/2, -z + 1$; #6 $-x, -y, -z$; #7 $x - 1/2, y + 1/2, z$; #8 $-x + 1/2, -y - 1/2, -z$.

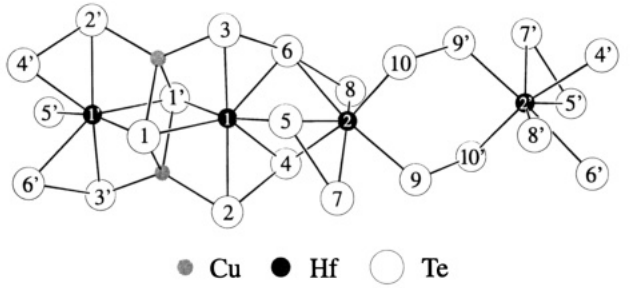

Figure 5. View of the anionic $^1_\infty[CuHf_2(Te_3)(Te_2)_3(Te)^{3-}]$ chain in $Cs_3CuHf_2Te_{10}$.

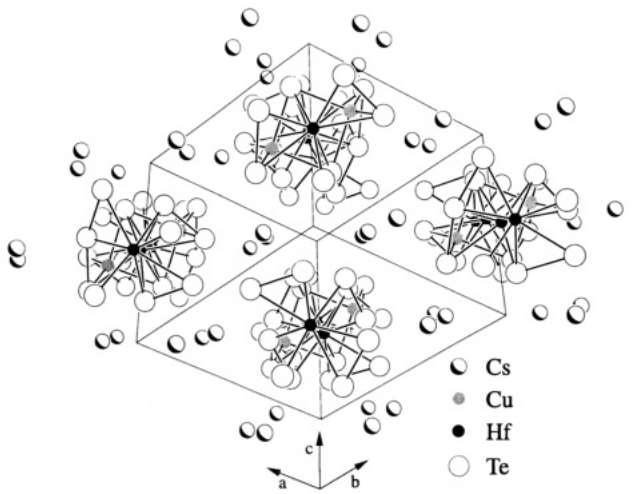

Figure 6. View of the unit cell of $Cs_3CuHf_2Te_{10}$.

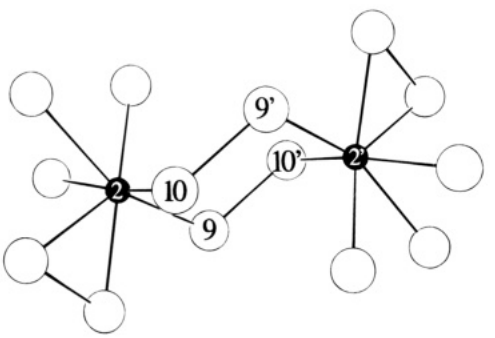

Figure 7. Six-membered Hf/Te ring in $Cs_3CuHf_2Te_{10}$.

octahedron is severely distorted, as the Te−Ti−Te angles range from 69.75(5) to 161.95(8)°.

Although $Cs_{0.68}CuTiTe_4$ represents a new structure type, it is closely related to the structures of the compounds $NaCuMQ_3$ (M = Ti, Zr; Q = S, Se, Te).[10] $Cs_{0.68}CuTiTe_4$ and $NaCuMQ_3$ contain CuQ_4 tetrahedra and MQ_6 octahedra. $NaCuMQ_3$ comprises $^2_\infty[CuMQ_3^-]$ layers with *pairs* of edge-shared CuQ_4 tetrahedra connected by edge-sharing to *pairs* of edge-shared MQ_6 octahedra. $Cs_{0.68}CuTiTe_4$ shows the same features, with one exception: the $TiTe_6$ octahedra do not edge share, but rather are connected through Te−Te bonds. This is illustrated in Figure 3 where a $^2_\infty[CuTiS_3^-]$ layer in $NaCuTiS_3$ is compared with a "layer" of $Cs_{0.68}CuTiTe_4$. The addition of the Te−Te bonds accounts for the difference in chalcogen stoichiometry between the two compounds. In the $ACuMQ_3$ series, the sum of the positive oxidation states is 6, as there is no Q−Q bonding. In $Cs_{0.68}CuTiTe_4$ this sum is reduced to 5.68, while the number of Te atoms in the formula unit

(30) Riekel, C.; Thomas, M.; Schöllhorn, R. *Phys. Status Solidi A* **1978**, *50*, K231−K234.

Table 5. Selected Bond Lengths (Å) and Angles (deg) for $Cs_3CuHf_2Te_{10}$[a]

Cu−Te(2)	2.543(4)
Cu−Te(3)#1	2.544(4)
Cu−Te(1)	2.692(4)
Cu−Te(1)#1	2.709(4)
Cu−Hf(1)#1	2.849(4)
Cu−Hf(1)	2.874(4)
Hf(1)−Te(4)	2.892(3)
Hf(1)−Te(2)	2.919(2)
Hf(1)−Te(5)	2.922(3)
Hf(1)−Te(6)	2.930(2)
Hf(1)−Te(3)	2.974(2)
Hf(1)−Te(1)	3.012(2)
Hf(2)−Te(8)	2.824(2)
Hf(2)−Te(9)	2.843(3)
Hf(2)−Te(10)	2.847(2)
Hf(2)−Te(5)	2.904(2)
Hf(2)−Te(7)	2.908(2)
Hf(2)−Te(4)	3.014(3)
Hf(2)−Te(6)	3.031(2)
Te(2)−Te(4)	2.810(3)
Te(3)−Te(6)	2.961(3)
Te(5)−Te(7)	2.768(3)
Te(6)−Te(8)	3.014(3)
Te(9)−Te(10)#2	2.801(3)
Te(2)−Cu−Te(3)#1	132.8(2)
Te(2)−Cu−Te(1)	94.52(13)
Te(3)#1−Cu−Te(1)	115.25(14)
Te(2)−Cu−Te(1)#1	115.66(14)
Te(3)#1−Cu−Te(1)#1	99.02(13)
Te(1)−Cu−Te(1)#1	93.30(12)
Te(1)#1−Hf(1)−Te(4)	95.88(6)
Te(1)#1−Hf(1)−Te(2)	100.75(6)
Te(4)−Hf(1)−Te(2)	57.84(6)
Te(1)#1−Hf(1)−Te(5)	168.05(7)
Te(4)−Hf(1)−Te(5)	92.84(6)
Te(2)−Hf(1)−Te(5)	90.81(6)
Te(1)#1−Hf(1)−Te(6)	93.90(6)
Te(4)−Hf(1)−Te(6)	78.76(6)
Te(2)−Hf(1)−Te(6)	135.15(7)
Te(5)−Hf(1)−Te(6)	79.78(6)
Te(1)#1−Hf(1)−Te(3)	98.71(7)
Te(4)−Hf(1)−Te(3)	137.08(7)
Te(2)−Hf(1)−Te(3)	153.67(7)
Te(5)−Hf(1)−Te(3)	69.36(6)
Te(6)−Hf(1)−Te(3)	60.19(6)
Te(1)#1−Hf(1)−Te(1)	84.02(6)
Te(4)−Hf(1)−Te(1)	138.02(7)
Te(2)−Hf(1)−Te(1)	80.84(7)
Te(5)−Hf(1)−Te(1)	94.94(6)
Te(6)−Hf(1)−Te(1)	143.21(7)
Te(3)−Hf(1)−Te(1)	83.74(7)
Te(8)−Hf(2)−Te(9)	91.68(7)
Te(8)−Hf(2)−Te(10)	108.28(7)
Te(9)−Hf(2)−Te(10)	94.97(7)
Te(8)−Hf(2)−Te(5)	138.57(7)
Te(9)−Hf(2)−Te(5)	127.38(7)
Te(10)−Hf(2)−Te(5)	84.12(6)
Te(8)−Hf(2)−Te(7)	148.36(7)
Te(9)−Hf(2)−Te(7)	71.76(6)
Te(10)−Hf(2)−Te(7)	100.06(7)
Te(5)−Hf(2)−Te(7)	56.88(6)
Te(8)−Hf(2)−Te(4)	69.28(7)
Te(9)−Hf(2)−Te(4)	96.31(7)
Te(10)−Hf(2)−Te(4)	168.52(7)
Te(5)−Hf(2)−Te(4)	90.72(6)
Te(7)−Hf(2)−Te(4)	85.54(6)
Te(8)−Hf(2)−Te(6)	61.85(6)
Te(9)−Hf(2)−Te(6)	153.53(7)
Te(10)−Hf(2)−Te(6)	93.55(7)
Te(5)−Hf(2)−Te(6)	78.41(7)
Te(7)−Hf(2)−Te(6)	131.04(7)
Te(4)−Hf(2)−Te(6)	75.34(6)

[a] Symmetry transformations used to generate equivalent atoms: #1 $-x, -y+1, -z+1$; #2 $-x+1, -y+2, -z$.

increases from 3 to 4 and Te–Te bonding is introduced. Atoms Te(3) and Te(4) are isolated Te^{2-} ions. If we consider Te(1)–Te(1′) to be a Te_2^{2-} unit, then 5 of the needed 5.68 negative charges are accounted for, and the remaining negative charge can be assigned to the Te(2) infinite chain (Te(2)–Te(2) = 2.923(1) Å). This chain resembles the infinite, linear chain found in $CsTiUTe_5$ (Te–Te = 3.065(1) Å).[31] Despite the short distances in the Te–Te chains along the needle axes in both materials, both are semiconductors, the conductivity in the needle (*b*) direction of the present compound being $5 \times 10^{-3}\ \Omega^{-1}\ cm^{-1}$ at room temperature.

$Cs_3CuHf_2Te_{10}$. $Cs_3CuHf_2Te_{10}$ has a new structure type within the family of quaternary A/group IV/Cu/Te compounds. While the metal coordination in this compound is common, the overall structure is unexpected. Similar quaternary chalcogenides[9,10] contain layers separated by alkali-metal cations, but $Cs_3CuHf_2Te_{10}$ comprises infinite one-dimensional chains of $HfTe_7$ polyhedra and edge-shared $CuTe_4$ tetrahedra (Figure 5) that are separated from one another by Cs^+ cations (Figure 6). Within a one-dimensional chain, atom Hf(1) is connected to atom Hf(2) through a face made up of atoms Te(4), Te(5), and Te(6). Hf(1) polyhedra are connected by edge sharing to edge-shared $CuTe_4$ tetrahedra. Finally atom Hf(2) is interconnected to atom Hf(2′) through an unusual six-membered ring consisting of the two Hf atoms and two Te–Te pairs (Te(9′)–Te(10) and Te(9)–Te(10′)). The six-membered Hf/Te ring is in the chair configuration, as seen in Figure 7. Insofar as we know, this unusual interconnection of the two group IV metal centers has not been observed before.

Selected distances and angles for $Cs_3CuHf_2Te_{10}$ are given in Table 5. Complete metrical data are given in Table SV.[25] The Cu–Te bond distances, which range from 2.543(4) to 2.709(4) Å, compare closely with those in Cu_2MTe_3 (2.594(1) to 2.705(1) Å).[12] The $CuTe_4$ tetrahedron is distorted, with Te–Cu–Te bond angles ranging from 94.52(13) to 132.8(2)°. The Hf–Te bond distances, which range from 2.824(2) to 3.031(2) Å, agree with those found in $K_4Hf_3Te_{17}$ (2.900(4) to 3.054(4) Å)[4] and Cu_2HfTe_3 (2.736(1) to 3.053(1) Å).[12]

As we have noted previously,[8] the designation of Te–Te "bonds" in these complex tellurides is often arbitrary. However, in the present structure there are only five short Te–Te pairs, ranging in length from 2.768(3) to 3.014(3) Å (Table 5). All other Te···Te contacts are >4.0 Å. If we consider these five short Te–Te pairs to be bonds, we can formulate the anion as $^1_\infty[CuHf_2(Te_3)(Te_2)_3(Te)^{3-}]$, although the assignment of formal oxidation states is not possible. In any event the material is an insulator or semiconductor, the conductivity in the needle [11$\bar{1}$] direction being $<1 \times 10^{-5}\ \Omega^{-1}\ cm^{-1}$ at room temperature.

Acknowledgment. This research was supported by NSF Grant No. DMR 91-14934. This work made use of MRL Central Facilities supported by the National Science Foundation at the Materials Research Center of Northwestern University under Grant No. DMR 91-20521.

Supplementary Material Available: Additional crystallographic details (Table SI), anisotropic displacement parameters (Tables SII and SIII), and bond lengths and angles (Tables SIV and SV) (18 pages). Ordering information is given on any current masthead page.

CM940502+

(31) Cody, J. A.; Ibers, J. A. *Inorg. Chem.*, in press.
(32) Huffman, J. C. Ph.D. Dissertation, Indiana University, 1974.